Chemical Science

ROYAL SOCIETY OF CHEMISTRY

EDGE ARTICLE

View Article Online
View Journal | View Issue

Check for updates

Cite this: *Chem. Sci.*, 2020, **11**, 11562

All publication charges for this article have been paid for by the Royal Society of Chemistry

Ruthenium-catalyzed cascade C–H activation/annulation of *N*-alkoxybenzamides: reaction development and mechanistic insight†

Liangliang Song,‡[a] Xiaoyong Zhang,‡[b] Xiao Tang,[c] Luc Van Meervelt,[d] Johan Van der Eycken,[e] Jeremy N. Harvey *[b] and Erik V. Van der Eycken *[af]

Received 12th August 2020
Accepted 26th September 2020

DOI: 10.1039/d0sc04434b

rsc.li/chemical-science

A highly selective ruthenium-catalyzed C–H activation/annulation of alkyne-tethered *N*-alkoxybenzamides has been developed. In this reaction, diverse products from inverse annulation can be obtained in moderate to good yields with high functional group compatibility. Insightful experimental and theoretical studies indicate that the reaction to the inverse annulation follows the Ru(II)–Ru(IV)–Ru(II) pathway involving N–O bond cleavage prior to alkyne insertion. This is highly different compared to the conventional mechanism of transition metal-catalyzed C–H activation/annulation with alkynes, involving alkyne insertion prior to N–O bond cleavage. *Via* this pathway, the *in situ* generated acetic acid from the N–H/C–H activation step facilitates the N–O bond cleavage to give the Ru-nitrene species. Besides the conventional mechanism forming the products *via* standard annulation, an alternative and novel Ru(II)–Ru(IV)–Ru(II) mechanism featuring N–O cleavage preceding alkyne insertion has been proposed, affording a new understanding of transition metal-catalyzed C–H activation/annulation.

Introduction

Transition metal-catalyzed C–H activation plays an important role in synthetic organic chemistry.[1] In particular, C–H activation followed by annulation with alkynes has emerged as an increasingly effective and attractive strategy for the construction of heterocycles and carbocycles in a step- and atom-economical manner.[2] In this regard, Rh(III)[3] or Ru(II)[4] catalysts have been employed in cascade C–H activation/annulation reactions with various types of alkynes, leading to the synthesis of isoquinolone derivatives through the use of external oxidants.

The utilization of internal oxidants exhibits a significant move forward in the area, avoiding the stoichiometric amount of external oxidants and potentially facilitating milder reactions.[5,6] For instance, the employment of a N–O bond as an internal oxidant is explored for the construction of isoquinolone analogues in Rh(III)- or Ru(II)-catalyzed C–H activation/annulation reactions and results in a number of examples, which indicated the potential of internal oxidizing directing groups in transition metal-catalyzed C–H activation. One such example was reported by Park,[5e] who described a rhodium(III)-catalyzed intramolecular annulation reaction of *N*-alkoxybenzamides to offer a new approach to isoquinolones (Scheme 1a). Subsequently, the internal oxidizing N–O bond has been used to synthesize structurally complex polycyclic compounds.[7] In 2014, Lin's group developed a Rh(III)-catalyzed arylative cyclization of *N*-hydroxybenzamides with cyclohexadienone-containing 1,6-enynes for the synthesis of tetracyclic isoquinolones.[7e] A Ru(II)-catalyzed regioselective intermolecular annulation of aryl substituted 2-acetylenic ketones with *N*-methoxybenzamides or acrylamides was reported by Chegondi in 2016.[7f] Recently, we demonstrated a Rh(III)-catalyzed sequential C(sp^2)–H activation and C(sp^3)–H amination for the preparation of polycyclic compounds (Scheme 1b).[7b,d]

Mechanistically (Scheme 2), these annulations have been explained in the light of an initial C–H activation to generate intermediate **I**, followed by alkyne insertion into the C–M bond leading to the seven-membered intermediate **II**, which delivers the isoquinolone products through sequential reductive

[a]*Laboratory for Organic & Microwave-Assisted Chemistry (LOMAC), Department of Chemistry, KU Leuven, Celestijnenlaan 200F, Leuven, 3001, Belgium. E-mail: erik.vandereycken@kuleuven.be*

[b]*Theoretical and Computational Chemistry, Department of Chemistry, KU Leuven, Celestijnenlaan 200F, Leuven, 3001, Belgium. E-mail: jeremy.harvey@kuleuven.be*

[c]*School of Chemistry, Physics and Mechanical Engineering, Queensland University of Technology, Gardens Point Campus, Brisbane, QLD 4001, Australia*

[d]*Biomolecular Architecture, Department of Chemistry, KU Leuven, Celestijnenlaan 200F, Leuven, 3001, Belgium*

[e]*Laboratory for Organic and Bio-Organic Synthesis, Department of Organic and Macromolecular Chemistry, Ghent University, Krijgslaan 281 (S.4), B-9000 Ghent, Belgium*

[f]*Peoples' Friendship University of Russia (RUDN University), Miklukho-Maklaya Street 6, Moscow, 117198, Russia*

† Electronic supplementary information (ESI) available. CCDC 1959807. For ESI and crystallographic data in CIF or other electronic format see DOI: 10.1039/d0sc04434b

‡ These authors contributed equally to this work.

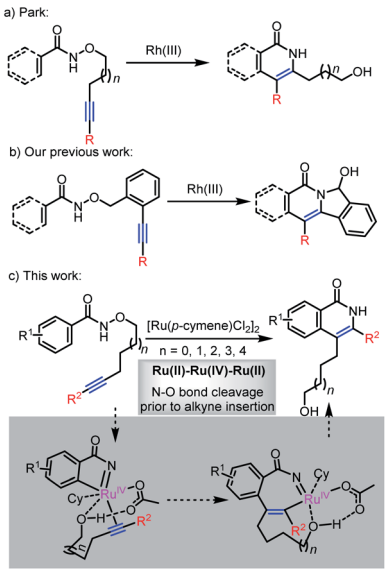

Scheme 1 Previous works and this approach.

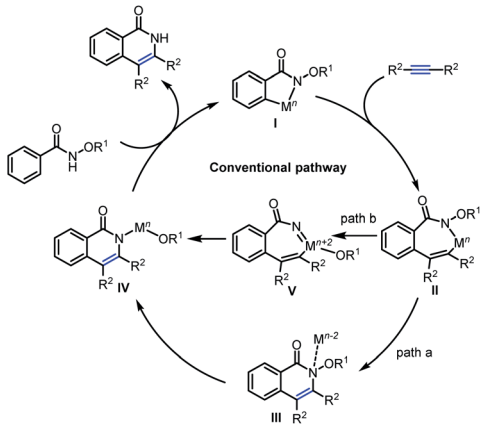

Scheme 2 Previously proposed catalytic cycle for C–H activation/annulation reactions.

elimination and oxidative addition into the N–O bond (path a, M^n–M^{n-2}–M^n pathway). Alternatively, intermediate **II** possibly undergoes oxidative addition into the N–O bond followed by reductive elimination to deliver the isoquinolones (path b, M^n–M^{n+2}–M^n pathway).[8] However, they are always restricted to alkyne insertion prior to N–O bond cleavage. Mechanistic investigations of the key intermediates in C–H activation/annulation processes are still somewhat limited, so it is not clear whether the mechanistic possibilities in Scheme 2 are sufficient to account for all observed reactivity in these systems. Formation of Rh(v) or Ru(iv) intermediates has been proposed from the experimental results,[9] but usually the mechanisms are assumed to involve alkyne insertion prior to N–O bond cleavage (path b). To the best of our knowledge, no unambiguous high-valent Cp*Rh(v) or (*p*-cymene)Ru(iv) complexes have been isolated to date, but DFT calculations have provided strong support for treating Rh(v) or Ru(iv) species as intermediates in reaction mechanisms.[10]

In comparison to previous hypotheses, we set out to investigate whether a catalytic cycle involving N–O bond cleavage prior to alkyne insertion might also play a role in some of these reactions.[11] The high-valent metal complex generated from N–O bond cleavage should increase the driving force for alkyne insertion and sequential reductive elimination (Scheme 1c). For this purpose, the ruthenium-catalyzed C–H activation/annulation of alkyne-tethered *N*-alkoxybenzamides is regarded as a platform for verifying this hypothesis.

Results and discussion

Reaction optimization

We initiated our studies with the exploration of the ruthenium-catalyzed C–H activation/annulation of alkyne-tethered *N*-alkoxybenzamide **1a**. To our delight, when **1a** was treated in the presence of $[Ru(p\text{-cymene})Cl_2]_2$ (10 mol%) and NaOAc (2 equiv.) in MeOH at 60 °C for 4 h, the product **3a** from inverse annulation was obtained in 81% yield, together with the product **2a** from standard annulation in 10% yield (Table 1, entry 1). Next various solvents were screened, such as DCE, CH_3CN, THF, acetone, 1,4-dioxane, toluene and DMF, and MeOH was identified as the preferred reaction medium (Table 1, entries 2–8). Adding PivOH (1 equiv.) did not improve the reaction (Table 1, entry 9). Replacing the additive NaOAc with CsOAc (2 equiv.) did not significantly influence the yield (Table 1, entry 10). The employment of $AgSbF_6$ (1 equiv.) instead of NaOAc completely inhibited the reaction (Table 1, entry 11). Decreasing the catalyst loading to 5 mol%, made the reaction much slower (Table 1,

Table 1 Optimization of the reaction conditions[a]

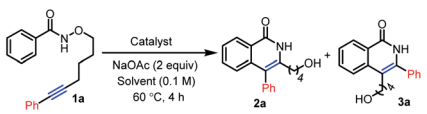

Entry	Catalyst	Solvent	2a[b] (%)	3a[b] (%)
1	**$[Ru(p\text{-cymene})Cl_2]_2$ (10 mol%)**	**MeOH**	**10**	**81**
2	$[Ru(p\text{-cymene})Cl_2]_2$ (10 mol%)	DCE	45	39
3	$[Ru(p\text{-cymene})Cl_2]_2$ (10 mol%)	CH_3CN	28	16
4	$[Ru(p\text{-cymene})Cl_2]_2$ (10 mol%)	THF	38	32
5	$[Ru(p\text{-cymene})Cl_2]_2$ (10 mol%)	Acetone	22	67
6	$[Ru(p\text{-cymene})Cl_2]_2$ (10 mol%)	1,4-Dioxane	32	19
7	$[Ru(p\text{-cymene})Cl_2]_2$ (10 mol%)	Toluene	42	29
8	$[Ru(p\text{-cymene})Cl_2]_2$ (10 mol%)	DMF	10	21
9[c]	$[Ru(p\text{-cymene})Cl_2]_2$ (10 mol%)	MeOH	12	76
10[d]	$[Ru(p\text{-cymene})Cl_2]_2$ (10 mol%)	MeOH	11	78
11[e]	$[Ru(p\text{-cymene})Cl_2]_2$ (10 mol%)	MeOH	0	0
12	$[Ru(p\text{-cymene})Cl_2]_2$ (5 mol%)	MeOH	6	43
13	$[Ru(C_6Me_6)Cl_2]_2$ (10 mol%)	MeOH	<5%	<5%
14	$[(C_6H_5)_3P]_3RuCl_2$ (20 mol%)	MeOH	<5%	<5%

[a] Condition: **1a** (0.3 mmol), $[Ru(p\text{-cymene})Cl_2]_2$, NaOAc (0.6 mmol), solvent (3.0 mL). [b] Isolated yield. [c] PivOH (1 equiv.) was added. [d] CsOAc (2 equiv.) instead of NaOAc. [e] $AgSbF_6$ (1 equiv.) instead of NaOAc.

entry 12). We also evaluated the performance of other Ru(II)-catalysts, such as $[Ru(C_6Me_6)Cl_2]_2$ and $[(C_6H_5)_3P]_3RuCl_2$ (Table 1, entries 13 and 14), but very low conversions were observed.

Examination of substrate scope

With the optimal reaction conditions in hand, we next investigated diverse substrates to evaluate the scope of the protocol (Table 2 and Scheme 3). Substrates with a wide range of electron-rich and -deficient groups at the *para* position of the benzamide proceeded smoothly to afford the products **3b–g** (67–85%) from inverse annulation (Table 2). The structure of **3c** has been confirmed by X-ray diffraction. In particular, the *meta*-methyl benzamide gave excellent regioselectivity in support of the sterically more accessible C–H bond, delivering product **3h** in 63% yield. The *ortho*-methyl-substituted derivative was also a productive substrate, leading to the product **3i** in 61% yield. The annulation reaction also worked well with electron-donating and -withdrawing groups in the aryl substituent of the alkyne, affording the products **3j–o** in 67–83% yield. When the aryl group of the alkyne was replaced by *n*-butyl group (Scheme 3), the products **2w** (59%) and **2x** (65%) from standard annulation were isolated as the main products, along with concomitant products **3w** (27%) and **3x** (31%) from inverse annulation. Moreover, only products **2y** and **2z** from standard annulation were obtained in 89% and 68% yield from the TMS-substituted derivative and the substrate bearing a terminal alkyne respectively (Scheme 3), while previous approaches[5e,7b]

Table 2 Scope for *N*-alkoxybenzamide substrates[a]

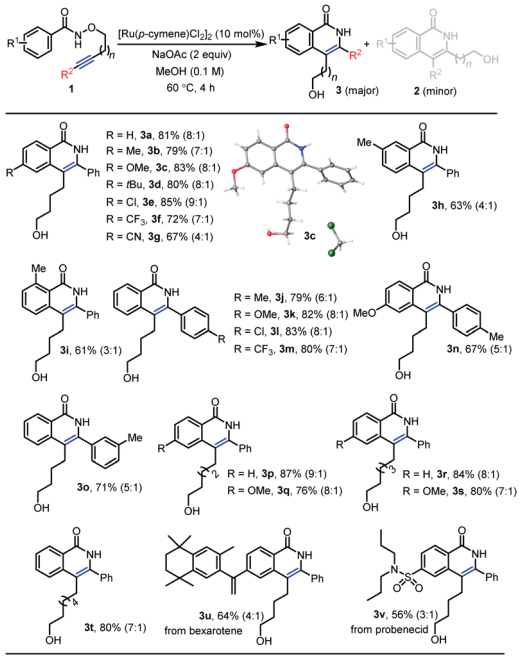

[a] Conditions: **1** (0.3 mmol), $[Ru(p\text{-cymene})Cl_2]_2$ (0.03 mmol), NaOAc (0.6 mmol) and MeOH (3.0 mL). **3** was isolated by column chromatography. The ratio of **3** : **2** shown in parenthesis was determined by ^1H NMR analysis of the crude reaction mixture.

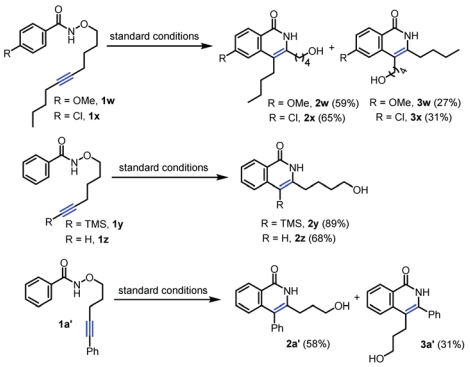

Scheme 3 Ruthenium-catalyzed C–H activation/annulation.

were limited to internal alkynes. Next, we evaluated the length of the tethers between the oxygen atom and the alkyne. Substrates with five-, six- and seven-carbon-atom tethers delivered the products **3p–t** from inverse annulation in 76–87% yield. The substrate with a three-carbon-atom tether delivered the product **2a′** (58%) from standard annulation as the main product, together with the product **3a′** from inverse annulation in 31% yield (Scheme 3). To further demonstrate the synthetic utility of this methodology, the annulation reaction was performed using *N*-alkoxybenzamides derived from the pharmaceuticals bexarotene and probenecid, resulting in the products **3u** (64%) and **3v** (56%) from inverse annulation.

Mechanistic studies

Based on above experimental results, three possible reaction pathways from conventional mechanism for the inverse annulation were firstly proposed. That is, intramolecular annulation *via* bridged Ru(II)-intermediate (Scheme 4a), or intermolecular annulation from cleavage products (Scheme 4b), or intermolecular version *via* homo-annulation (Scheme 4c). To gain more mechanistic insight of the present reaction, a series of control

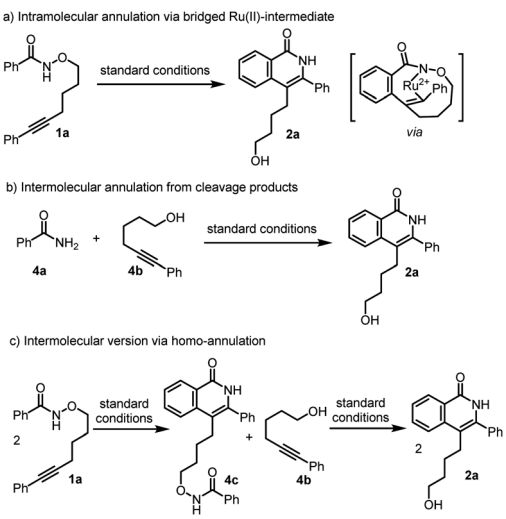

Scheme 4 Possible mechanisms from initial assumption.

experiments were performed. Reversibility experiments concerning the C–H activation step, using **1a** in the presence of deuterated methanol (Scheme 5a), showed that there is no deuterium incorporation in the recovered substrate and products, which indicates that the C–H activation step is irreversible. To further investigate the C–H activation process, kinetic isotope effect (KIE) experiments were performed (Scheme 5b). The competitive experiment gave $k_H/k_D = 1.1$ for the formation of **3a** and $k_H/k_D = 1.0$ for the formation of **2a**, while the parallel experiment delivered $k_H/k_D = 1.4$ for the formation of **3a** and $k_H/k_D = 1.5$ for the formation of **2a**, clearly indicating that the C–H bond cleavage process is not involved in the rate-limiting step, which is different from Park's work.[5e] When **1a** was treated under $[Ru(p\text{-cymene})Cl_2]_2$ (5 mol%) at r.t. for 0.5 h (Scheme 5c), the product **3a** and alcohol **4b** were obtained in 5% and 2% yields respectively, while only <1% product **2a** and trace amount of benzamide **4a** were detected. We did not observe the formation of compound **4c**. When benzofuran substrate **5** was employed under the standard conditions, the product **6b** from inverse annulation was isolated in 20%, together with the product **6c** (29%) from standard annulation, benzamide **6a** (33%) and alcohol **4b** (31%) (Scheme 5d). The isolation of cleavage products amide and alcohol as well as no compound **4c** formed, suggest that the N–O bond cleavage occurs prior to the alkyne insertion. Therefore, pathways in Scheme 4a and c can be ruled out. Also, from DFT calculation results, pathway in Scheme 4a is less favorable (see ESI†).[12d] We also did the crossing experiment of **1c** and **1j** under the standard conditions (Scheme 5e), resulting in four annulation products. This result further indicates that the N–O bond cleavage occurs prior to the alkyne insertion. Under the standard conditions, the reaction of **4a** and **4b** could not deliver the annulation products (Scheme 5f), and only minor amount of product **3a** was obtained when $Cu(OAc)_2$ (2 equiv.) was added. This indicates that the formation of **2a** and **3a** does not follow the pathway involving **4a** and **4b** from the cleavage of **1a**. Thus pathway in Scheme 4b can be ruled out.

To provide more light on the formation of annulation products, DFT calculations employing B3LYP-D3/def2-TZVP method were performed with the $Ru(OAc)_2(p\text{-cymene})$ catalyst **A** and the three-carbon-atom (**1a′**) tether substrate. We first consider the previously proposed Ru(II)–Ru(0)–Ru(II) mechanism (Scheme 6),[5e,7,10] which involves an initial two-step C–H activation (**TS1**), followed by the rate-determining step (RDS), alkyne insertion through **TS2**. These steps are followed by

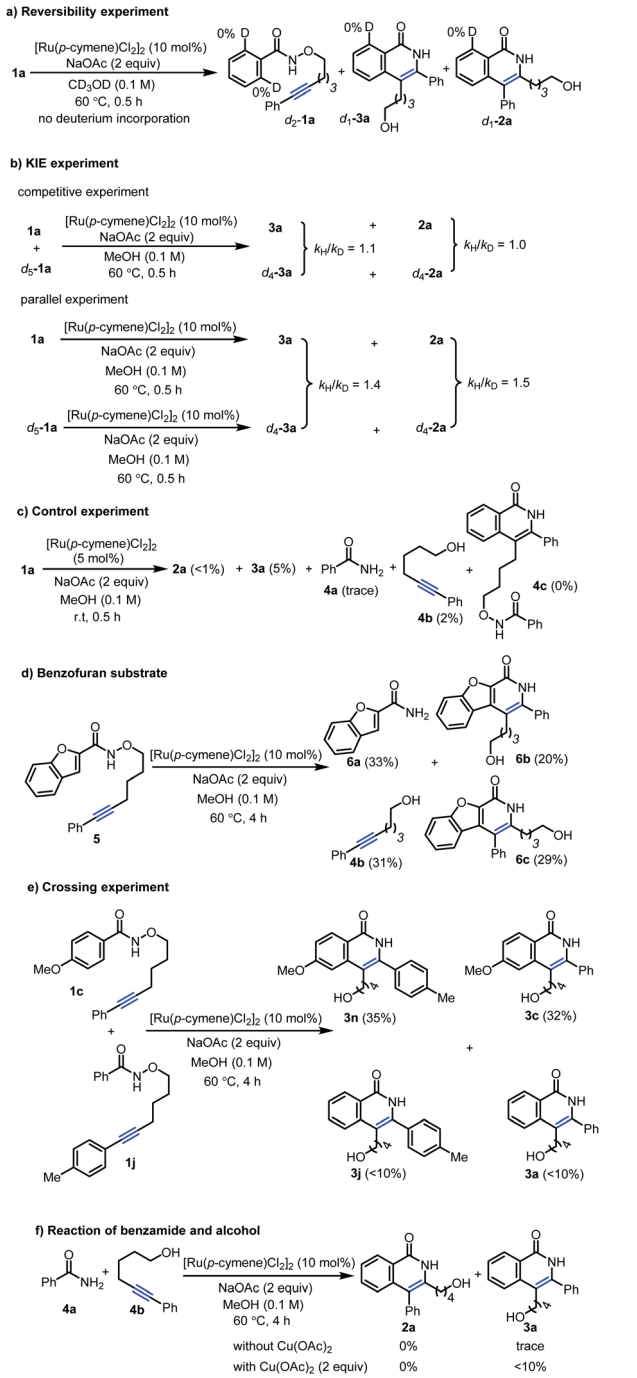

Scheme 5 Control experiments and deuterium-labeling experiments.

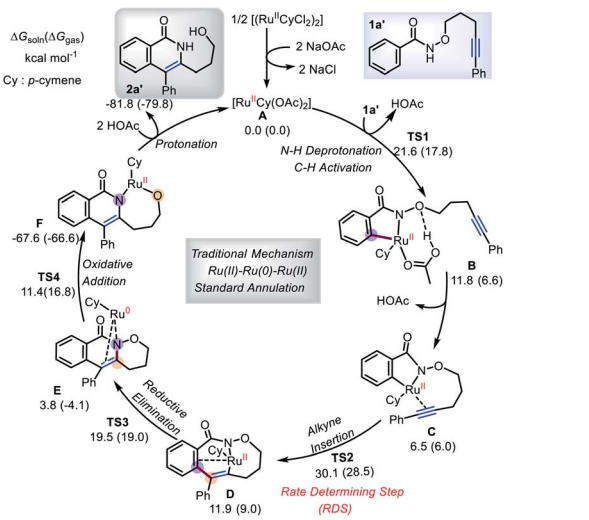

Scheme 6 Traditional mechanistic cycle leading to the standard annulation product. Computed relative free energies (kcal mol^{-1}, B3LYP-D3/def2-TZVP (SMD : methanol)).

reductive elimination (**TS3**) and N–O oxidative cleavage (**TS4**). The overall free energy barrier is 28.5–30.1 kcal mol^{-1}, and only the product **2a′** from the standard annulation reaction can be formed.[12]

Based on the experimental observations and DFT calculations, we then propose an alternative competitive Ru(II)–Ru(IV)–Ru(II) mechanism (Scheme 7) featuring N–O cleavage preceding alkyne insertion, which can lead to formation of both the standard **2a′** and inverse **3a′** annulation products. As in the previous mechanism, the first steps are N–H deprotonation and C–H activation (**TS1**, 17.8–21.6 kcal mol^{-1}) forming metallacycle **B**. At this point, as well as the previously suggested alkyne insertion, the system can undergo an acid-assisted N–O cleavage process (**TS5**, 27.2–31.7 kcal mol^{-1}) to afford the Ru(IV)-nitrene species **G** (4.5–5.5 kcal mol^{-1}), in which the forming alcohol (5-phenylpent-4-yn-1-ol) is H-bonded to the acetate ligand. Dissociation of alcohol from **G** is weakly endergonic by 1.8 kcal mol^{-1} in solution relative to **A**, consistent with the experimental observation of small amounts of alcohol side-product. The N–O cleavage is strongly acid-assisted: in the absence of HOAc, the barrier to this process is much higher (**TS10**, 50.1–54.6 kcal mol^{-1} in Scheme 8a), while **TS2** is acid-insensitive.[12a] Analysis of the electronic structure of the **TS** indicates that this is because this step is a direct heterolytic cleavage between two atoms with small electronegativity difference (Scheme 8b). Natural population analysis (NPA) shows that the alkoxyl oxygen atom in **TS10** has a large negative charge ($-0.71e$), which can be stabilized by proton transfer in **TS5**, and the resulting acetate base could delocalize the negative charge.[13] These results suggest that the *in situ* generated acetic acid from N–H/C–H activation step could serve to facilitate the N–O bond cleavage.

Further coordination of the alkyne fragment in 5-phenylpent-4-yn-1-ol to the metal from intermediate **G** is very exothermic and can form two different Ru(IV) intermediates (Scheme 7), **H1** and **H2**, which differ based on the orientation of the phenyl substituent of 5-phenylpent-4-yn-1-ol. They thereby lead to different annulation products, with **H1** forming **2a′**, while **H2** yields **3a′**, in each case through a sequence of steps involving alkyne insertion (**TS6**/**TS8**), reductive elimination (**TS7**/**TS9**) and protonation. The corresponding barriers are much smaller than that of the N–O cleavage process,[14] and similar in the standard annulation case, consistent with the observation of both types of annulation products.

The **TS** of the RDS step (acid-assisted N–O cleavage process, **TS5**) in the present Ru(II)–Ru(IV)–Ru(II) mechanism (Scheme 7) is only slightly different in free-energy to that of the key **TS** (for alkyne insertion, **TS2**) in the traditional Ru(II)–Ru(0)–Ru(II) mechanism (Scheme 6), which makes it difficult to determine solely from computation which mechanism should be dominant, especially as the relative free energies are somewhat sensitive to the nature of the density functional used in the computations (see ESI†). In additional calculations with the four-carbon-atom tethered substrate, the two mechanisms are also found to have similar activation free energies (Scheme 8c). For both the three- (**1a′**) and four-carbon-atom (**1a**) tethered substrates, **TS5** is lower (by 1.3 kcal mol^{-1}, and 4.0 kcal mol^{-1}, respectively) in the gas phase free energy, but relatively higher (by 1.6 kcal mol^{-1}, and 0.6 kcal mol^{-1}, respectively) in the solution phase free energy than **TS2**. In experiments, reaction with **1a′** yields more standard annulation product **2a′** (58%) than the inverse annulation product **3a′** (31%), while reaction with **1a** leads to more inverse annulation product **3a** (81%) and less standard annulation product **2a** (10%). The calculated slightly lower solution phase free energies for **TS2** than for **TS5**

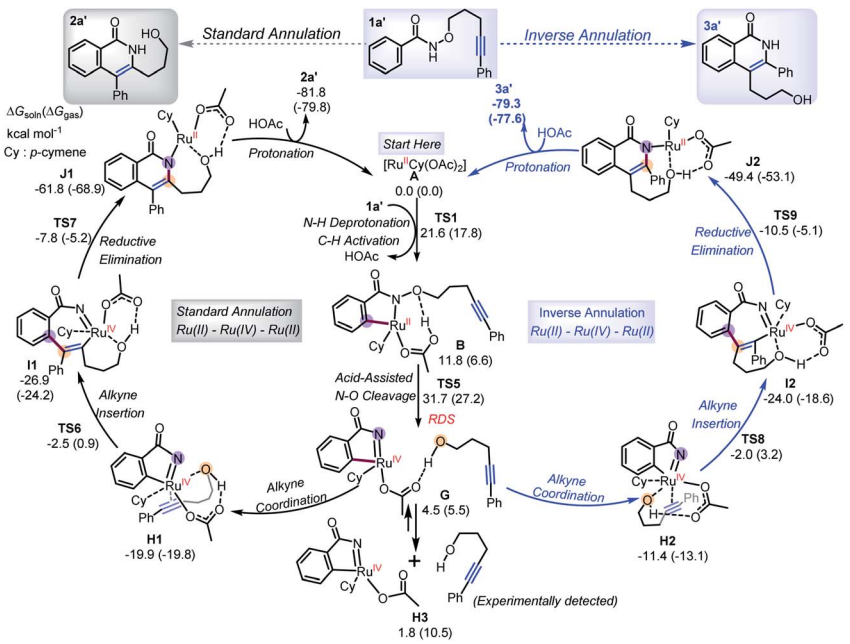

Scheme 7 New suggested mechanism. Computed relative free energies (kcal mol^{-1}, B3LYP-D3/def2-TZVP (SMD : methanol)).

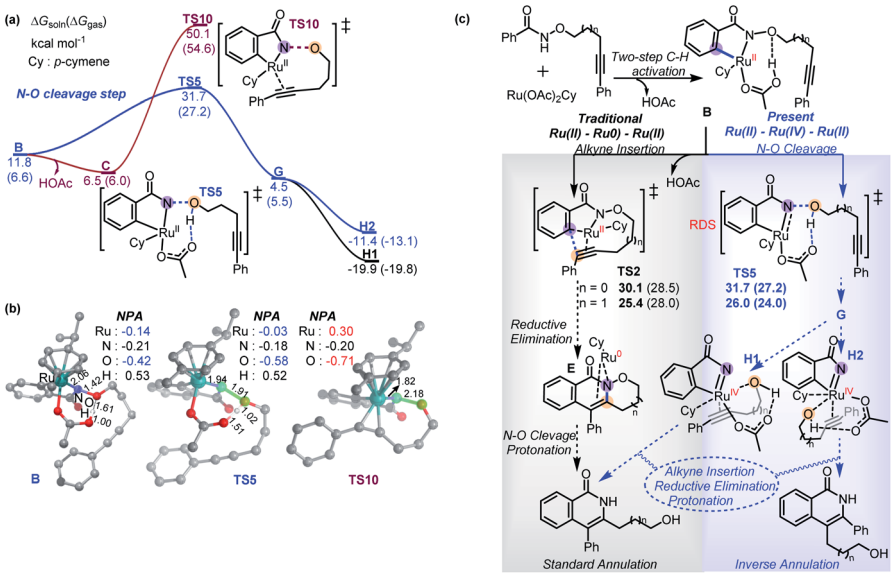

Scheme 8 Role of acetic acid in the N–O cleavage. (a) Energy profiles (kcal mol^{-1}) for the N–O cleavage step in the Ru(II)–Ru(IV)–Ru(II) pathway. (b) Structures of the N–O cleavage transition states, including NPA charges of key atoms and selected interatomic distances (in Å). (c) Schematics pathways for Ru-catalyzed annulation reaction.

should make the traditional mechanism, and thereby the standard annulation product, dominant in both cases. However, given the small calculated energy difference and the expected error bars (the two **TS**s differ significantly in electronic structure, so favorable error compensation cannot be expected), our results are consistent with the new mechanism *via* **TS5** playing an important role. Therefore, our DFT calculations combined with experimental observations suggest that formation of the inverse annulation products follows the Ru(II)–Ru(IV)–Ru(II) cycle, while the "standard" annulation products could be formed by either the Ru(II)–Ru(0)–Ru(II) or Ru(II)–Ru(IV)–Ru(II) mechanism, or both.

Conclusions

In summary, we have developed a ruthenium-catalyzed C–H activation/annulation process of alkyne-tethered *N*-alkoxybenzamides with high selectivity. This methodology is compatible with various kinds of *N*-alkoxybenzamides including bexarotene and probenecid derivatives, providing a wide range of products from inverse annulation. Detailed experimental investigations and DFT calculations reveal that the inverse annulation follows a Ru(II)–Ru(IV)–Ru(II) mechanism featuring N–O cleavage preceding alkyne insertion. Formation of the putative Ru-nitrene intermediate is assisted by the *in situ* generated acetic acid from N–H/C–H activation step. Formation of the standard annulation products might follow either the traditional Ru(II)–Ru(0)–Ru(II) pathway involving alkyne insertion prior to N–O bond cleavage, or the newly proposed Ru(II)–Ru(IV)–Ru(II) mechanism featuring N–O cleavage preceding alkyne insertion. The balance between the two mechanisms and between the inverse and standard routes will depend on the catalyst (*e.g.* Rh(III) *vs.* Ru(II)), the nature of the substrate (alkyl chain or benzylidene linker) and other factors (*e.g.*, solvents, additives). Kinetic studies and theoretical studies suggest that C–H bond cleavage process is not involved in the rate-limiting step.

Conflicts of interest

There are no conflicts to declare.

Acknowledgements

Liangliang Song appreciates the Postdoctoral Mandate (PDM) of KU Leuven. Xiaoyong Zhang appreciates the China Scholarship Council (CSC) for providing a doctoral scholarship. LVM thanks the Hercules Foundation for supporting the purchase of the diffractometer through project AKUL/09/0035. We acknowledge the FWO [Fund for Scientific Research-Flanders (Belgium)] and the Research Council of KU Leuven (BOF) for financial support. We acknowledge the support of RUDN University Program 5-100. The computational resources and services used in this work are provided by the VSC (Flemish Supercomputer Center), funded by the Research Foundation-Flanders (FWO) and the Flemish Government-department EWI.

Notes and references

1 For selected reviews on catalytic C–H bond activation, see: (*a*) J. He, M. Wasa, K. S. Chan, Q. Shao and J.-Q. Yu, *Chem. Rev.*, 2016, **117**, 8754; (*b*) K. Murakami, S. Yamada, T. Kaneda and K. Itami, *Chem. Rev.*, 2017, **117**, 9302; (*c*) J. C. Chu and T. Rovis, *Angew. Chem., Int. Ed.*, 2018, **57**, 62; (*d*) P. Gandeepan, T. Müller, D. Zell, G. Cera, S. Warratz and L. Ackermann, *Chem. Rev.*, 2018, **119**, 2192; (*e*) Y. Park,

Y. Kim and S. Chang, *Chem. Rev.*, 2017, **117**, 9247; (*f*) G. Rouquet and N. Chatani, *Angew. Chem., Int. Ed.*, 2013, **52**, 11726; (*g*) X.-S. Zhang, K. Chen and Z.-J. Shi, *Chem. Sci.*, 2014, **5**, 2146; (*h*) N. Kuhl, N. Schroeder and F. Glorius, *Adv. Synth. Catal.*, 2014, **356**, 1443.

2 For reviews, see: (*a*) G. Song, F. Wang and X. Li, *Chem. Soc. Rev.*, 2012, **41**, 3651; (*b*) T. Satoh and M. Miura, *Chem.–Eur. J.*, 2010, **16**, 11212; (*c*) L. Ackermann, *Acc. Chem. Res.*, 2014, **47**, 281; (*d*) M. Gulías and J. L. Mascareñas, *Angew. Chem., Int. Ed.*, 2016, **55**, 11000; (*e*) Y. Yang, K. Li, Y. Cheng, D. Wan, M. Li and J. You, *Chem. Commun.*, 2016, **52**, 2872; (*f*) S. Prakash, R. Kuppusamy and C.-H. Cheng, *ChemCatChem*, 2018, **10**, 683.

3 For rhodium-catalyzed annulation with external oxidants, see: (*a*) S. Mochida, N. Umeda, K. Hirano, T. Satoh and M. Miura, *Chem. Lett.*, 2010, **39**, 744; (*b*) T. K. Hyster and T. Rovis, *J. Am. Chem. Soc.*, 2010, **132**, 10565; (*c*) G. Song, D. Chen, C.-L. Pan, R. H. Crabtree and X. Li, *J. Org. Chem.*, 2010, **75**, 7487; (*d*) N. S. Upadhyay, V. H. Thorat, R. Sato, P. Annamalai, S.-C. Chuang and C.-H. Cheng, *Green Chem.*, 2017, **19**, 3219; (*e*) L. Song, G. Tian, Y. He and E. V. Van der Eycken, *Chem. Commun.*, 2017, **53**, 12394; (*f*) P. Tao and Y. Jia, *Chem. Commun.*, 2014, **50**, 7367; (*g*) J. Zheng, S. B. Wang, C. Zheng and S. L. You, *Angew. Chem.*, 2017, **129**, 4611; (*h*) J. Li, J. Liu, J. Yin, Y. Zhang, W. Han, J. Lan, D. Wu, Z. Bin and J. You, *J. Org. Chem.*, 2019, **84**, 15697; (*i*) L. Song, G. Tian, A. Blanpain, L. Van Meervelt and E. V. Van der Eycken, *Adv. Synth. Catal.*, 2019, **361**, 4442.

4 For ruthenium-catalyzed annulation with external oxidants, see: (*a*) L. Ackermann, A. V. Lygin and N. Hofmann, *Angew. Chem., Int. Ed.*, 2011, **50**, 6379; (*b*) L. Ackermann, A. V. Lygin and N. Hofmann, *Org. Lett.*, 2011, **13**, 3278; (*c*) R. P. Tulichala, M. Shankar and K. K. Swamy, *J. Org. Chem.*, 2017, **82**, 5068; (*d*) H. Lin, S.-S. Li and L. Dong, *Org. Biomol. Chem.*, 2015, **13**, 11228; (*e*) D. N. Garad and S. B. Mhaske, *J. Org. Chem.*, 2019, **84**, 1863.

5 For rhodium-catalyzed annulation with internal oxidants, see: (*a*) N. Guimond, C. Gouliaras and K. Fagnou, *J. Am. Chem. Soc.*, 2010, **132**, 6908; (*b*) N. Guimond, S. I. Gorelsky and K. Fagnou, *J. Am. Chem. Soc.*, 2011, **133**, 6449; (*c*) S. Rakshit, C. Grohmann, T. Besset and F. Glorius, *J. Am. Chem. Soc.*, 2011, **133**, 2350; (*d*) H. Wang, C. Grohmann, C. Nimphius and F. Glorius, *J. Am. Chem. Soc.*, 2012, **134**, 19592; (*e*) X. Xu, Y. Liu and C. M. Park, *Angew. Chem., Int. Ed.*, 2012, **51**, 9372; (*f*) L. Song, G. Tian and E. V. Van der Eycken, *Mol. Catal.*, 2018, **459**, 129; (*g*) X. Wu, B. Wang, Y. Zhou and H. Liu, *Org. Lett.*, 2017, **19**, 1294; (*h*) S. Lee, N. Semakul and T. Rovis, *Angew. Chem., Int. Ed.*, 2020, **59**, 4965; (*i*) M. Xu, C. Wang, W. Jiang and B. Xiao, *Adv. Synth. Catal.*, 2020, **362**, 1706; (*j*) T. J. Saiegh, H. Chédotal, C. Meyer and J. Cossy, *Org. Lett.*, 2019, **21**, 8364; (*k*) E. Tan, O. Quinonero, M. Elena de Orbe and A. M. Echavarren, *ACS Catal.*, 2018, **8**, 2166; (*l*) H. Gao, M. Sun, H. Zhang, M. Bian, M. Wu, G. Zhu, Z. Zhou and W. Yi, *Org. Lett.*, 2019, **21**, 5229; (*m*) T. Yamada, Y. Shibata, S. Kawauchi, S. Yoshizaki and K. Tanaka, *Chem.–Eur. J.*, 2018, **24**, 5723; (*n*) J. F. Tan, C. T. Bormann, K. Severin and N. Cramer, *ACS Catal.*, 2020, **10**, 3790; (*o*) W. J. Cui, Z. J. Wu, Q. Gu and S. L. You, *J. Am. Chem. Soc.*, 2020, **142**, 7379.

6 For ruthenium-catalyzed annulation with internal oxidants, see: (*a*) B. Li, H. Feng, S. Xu and B. Wang, *Chem.–Eur. J.*, 2011, **17**, 12573; (*b*) L. Ackermann and S. Fenner, *Org. Lett.*, 2011, **13**, 6548; (*c*) H. Huang, S. Nakanowatari and L. Ackermann, *Org. Lett.*, 2017, **19**, 4620; (*d*) X. Wu, B. Wang, S. Zhou, Y. Zhou and H. Liu, *ACS Catal.*, 2017, **7**, 2494; (*e*) F. Yang and L. Ackermann, *J. Org. Chem.*, 2014, **79**, 12070; (*f*) E. Tan, A. I. Konovalov, G. A. Fernández, R. Dorel and A. M. Echavarren, *Org. Lett.*, 2017, **19**, 5561.

7 (*a*) S. Y. Hong, J. Jeong and S. Chang, *Angew. Chem., Int. Ed.*, 2017, **56**, 2408; (*b*) L. Song, X. Zhang, G. Tian, K. Robeyns, L. Van Meervelt, J. N. Harvey and E. V. Van der Eycken, *Mol. Catal.*, 2019, **463**, 30; (*c*) Y. Fukui, P. Liu, Q. Liu, Z.-T. He, N.-Y. Wu, P. Tian and G.-Q. Lin, *J. Am. Chem. Soc.*, 2014, **136**, 15607; (*d*) L. Song, G. Tian, J. Van der Eycken and E. V. Van der Eycken, *Beilstein J. Org. Chem.*, 2019, **15**, 571; (*e*) J.-P. Krieger, D. Lesuisse, G. Ricci, M.-A. Perrin, C. Meyer and J. Cossy, *Org. Lett.*, 2017, **19**, 2706; (*f*) K. K. Gollapelli, S. Kallepu, N. Govindappa, J. B. Nanubolu and R. Chegondi, *Chem. Sci.*, 2016, **7**, 4748; (*g*) M. Shankar, K. Ghosh, K. Mukherjee, R. K. Rit and A. K. Sahoo, *Org. Lett.*, 2018, **20**, 5144.

8 (*a*) J.-Q. Wu, S.-S. Zhang, H. Gao, Z. Qi, C.-J. Zhou, W.-W. Ji, Y. Liu, Y. Chen, Q. Li, X. Li and H. Wang, *J. Am. Chem. Soc.*, 2017, **139**, 3537; (*b*) X. Wang, T. Gensch, A. Lerchen, C. G. Daniliuc and F. Glorius, *J. Am. Chem. Soc.*, 2017, **139**, 6506; (*c*) S. H. Park, J. Kwak, K. Shin, J. Ryu, Y. Park and S. Chang, *J. Am. Chem. Soc.*, 2014, **136**, 2492; (*d*) Y. F. Liang, L. Yang, T. Rogge and L. Ackermann, *Chem.–Eur. J.*, 2018, **24**, 16548; (*e*) M. Simonetti, D. M. Cannas, X. Just-Baringo, I. J. Vitorica-Yrezabal and I. Larrosa, *Nat. Chem.*, 2018, **10**, 724.

9 (*a*) C. Q. Wang, Y. Zhang and C. Feng, *Angew. Chem., Int. Ed.*, 2017, **56**, 14918; (*b*) Z. Zhou, G. Liu, Y. Shen and X. Lu, *Org. Chem. Front.*, 2014, **1**, 1161.

10 (*a*) S. Vasquez-Cespedes, X. Wang and F. Glorius, *ACS Catal.*, 2018, **8**, 242; (*b*) Z. Wang, P. Xie and Y. Xia, *Chin. Chem. Lett.*, 2018, **29**, 47; (*c*) G. Duarah, P. P. Kaishap, T. Begum and S. Gogoi, *Adv. Synth. Catal.*, 2019, **361**, 654; (*d*) L. Xu, Q. Zhu, G. Huang, B. Cheng and Y. Xia, *J. Org. Chem.*, 2012, **77**, 3017; (*e*) B. Ling, Y. Liu, Y.-Y. Jiang, P. Liu and S. Bi, *Organometallics*, 2019, **38**, 1877; (*f*) Y.-F. Yang, K. N. Houk and Y.-D. Wu, *J. Am. Chem. Soc.*, 2016, **138**, 6861.

11 (*a*) S. Huh, S. Y. Hong and S. Chang, *Org. Lett.*, 2019, **21**, 2808; (*b*) E. Azek, M. Khalifa, J. Bartholoméüs, M. Ernzerhof and H. Lebel, *Chem. Sci.*, 2019, **10**, 718.

12 (*a*) In the traditional mechanism, the acetic acid has a negligible effect on the barrier height of the rate determining alkyne insertion step, since **TS2** in the presence of acid (Scheme S2 in ESI†) is calculated to be 30.7 kcal mol^{-1}, comparable to the one (30.1 kcal mol^{-1}) in the absence of acid; (*b*) The pathway with alkyne insertion into the Ru–N bond prior to C–C reductive elimination is less favorable with a barrier of 35.4 kcal mol^{-1}; (*c*) After alkyne insertion into the Ru–C

bond, the pathway with N–O oxidative cleavage prior to reductive elimination involves **TS13** and **TS14** (>23.2 kcal mol^{-1}), higher in energy than **TS3** (19.5 kcal mol^{-1}) and **TS4**; (*d*) Alkyne insertion following the intramolecular annulation to inverse annulation product is calculated to involve a transition state more than 10.0 kcal mol^{-1} (Scheme S13†) higher than that to standard annulation product. Thus, the formation of inverse annulation product cannot be explained by the tradition mechanism. More details can be found in ESI.†

13 The effect of methanol was explicitly considered in the N–O cleavage step. In absence of acetic acid, the methanol could also transfer its hydrogen to neutralize alkoxyl oxygen atom of the substrate, and result into a negative methoxyl group. However, the calculated barrier is much higher (>46.9 kcal mol^{-1}) than that of the acetic acid assisted mechanism (Scheme S9†), which could be explained by the stronger acid of acetic acid to promote proton transfer, and the more stabilization of negative charge in the carboxylate group.

14 In the new suggested mechanism, once N–O cleavage completes, the barriers of alkyne insertion and reductive elimination in the absence of the acetic acid are at least 6.0 kcal mol^{-1} higher in energy (ESI, Scheme S11†), than that of the route (**H2** to **J2** in Scheme 6) in the presence of the acetic acid.